Worldwide theoretical comparison of outdoor potential for various silicon-based tandem module architectures

Haohui Liu[1], Carlos D. Rodríguez-Gallegos[2], Zhe Liu[3], Tonio Buonassisi[3], Thomas Reindl[2], and Ian Marius Peters[4]

[1]Envision Digital International, 098632, Singapore
[2]Solar Energy Research Institute of Singapore, National University of Singapore, 117574, Singapore
[3]Massachusetts Institute of Technology, Cambridge, MA, 02139, USA
[4]Forschungszentrum Jülich GmbH, 91058 Erlangen, Germany

***Abstract*— Non-concentrating tandem solar are on the verge of entering the PV market. One particular challenge for tandem solar cells is the interconnection scheme of the sub-cells in a module, and the implications on techno-economic factors. Here, we theoretically compare four possible tandem module architectures using the material combinations GaAs and perovskite on silicon to their single-junction counterparts. We model energy yield and performance ratios for operating conditions around the globe, and we explore the differences in cost structures. In general, we find the techno-economic performance of three-terminal and mechanically voltage-matched modules to be the most promising. Tandems are especially well suited for high-value markets and arid climates. In such conditions, the manufacturing cost premium for a record-level tandem is up to three times that of a silicon PV module.**

Keywords*— Si-based tandem; tandem architecture; outdoor performance; performance ratio; LCOE; worldwide; two-terminal; areal-matched; four-terminal; three-terminal; voltage-matched

I. Introduction

Recently, Si based flat-panel tandem solar cells have advanced, with cell efficiencies exceeding the important milestone of 30% for III-V on silicon technology [1] and approaching 30% for perovskite on silicon technology [2]. Commercialization of tandems will require module integration of the cells, which for tandems is particular because of the need to interconnect the different sub-cells and the various interconnection schemes this allows. There are multiple ways to integrate the top and bottom cells of a tandem solar cell into a module. Generally, the following architectures are possible (Figure 1): two-terminal (2T), areal-matched (AM) [3], four-terminal (4T), mechanically voltage-matched (VM) [4-6], and three-terminal (3T) [7–12]. More configurations and combinations of architectures can be realized, though they will follow one or several of these basic architectures. While many studies have explored the efficiency and cost of lab-scale tandem solar cells, the impact of different module architectures on yield and techno-economic performance in different operating conditions and locations is still a scarcely explored topic.

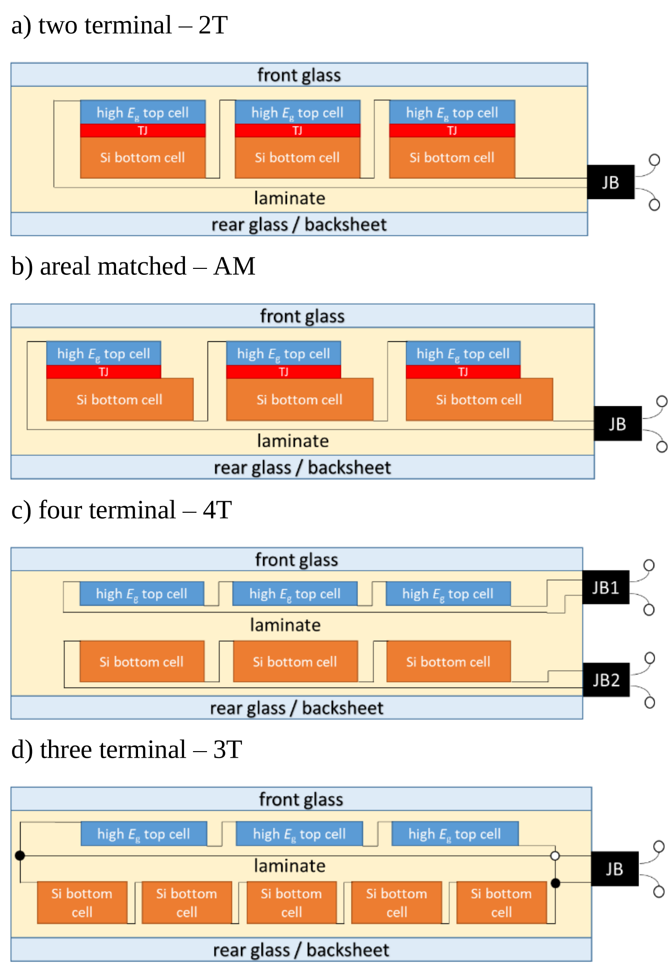

Figure 1. Conceptual tandem module configurations explored in this study. Figures haven been adapted from [13]. Note that the 3T and the voltage matched tandem module behave similarly. We only show results for 3T here.

In this paper, we explore the techno-economic performance of the various tandem module architectures in different climates from the perspective of outdoor performance ratio and implied

LCOE. We extend previous yield studies with a comprehensive geographical coverage, a more complete set of material systems, and more suitable device models to predict and compare the behavior of different tandem PV module architectures and to compare to single-junction alternatives. These results help guide the evaluation of future designs of commercial tandem modules and their cost targets. For system designers and the broader industry, these results offer a preliminary assessment on the practical viability of flat-plate tandem technology in different parts of the world.

II. Methodology

A. Tandem module architectures

The characteristics of five basic tandem module architectures, as shown in Figure 1, are summarized in Table 1. The optical absorption in the sub-cells are calculated using measured sub-cell external quantum efficiencies (EQE) of record tandem solar cells from literature. Electrical properties of high quality, record-level sub-cells are assumed for each tandem configuration.

TABLE I. **Configurations investigated in this work for each architecture**

Configuration (tandem or SJ)	*STC efficiency (%)*	*Maximum Yield [kWh/m²]*
2T GaAs-Si	29.2	582
3T GaAs-Si	33.0	651
4T GaAs-Si	34.2	677
AM GaAs-Si	31.3	620
VM GaAs-Si	33.9	669
2T perovskite-Si	30.8	631
3T perovskite-Si	25.6	525
4T perovskite-Si AM	27.5	566
perovskite-Si VM	27.3	553
perovskite-Si	27.4	565
Si (PERC)	21.3	540
GaAs	28.1	550
Perovskite	21.7	443

Tandem device output is modelled using a coupled optoelectronic model taking photon recycling and luminescent coupling (LC) into consideration. We adopted the optoelectronic model from Geisz et al [14] for this purpose. Optical absorption and current generation under arbitrary incoming spectra are calculated primarily by folding experimentally measured cell / sub-cell external quantum efficiency (EQE) with the spectrum. The exception is the 2T GaAs on Si configuration, for which no reliable measurement was available. For this case, QE was calculated via optical simulation coupling the transfer matrix method and ray tracing using a method developed by Liu et al [15]. With the calculated photogeneration current density in the SJ solar cell or each sub-cell in a tandem, the individual IV curves are simulated, assuming electrical properties corresponding to record cell performance. IV curves are then corrected using a linear temperature coefficient model. The model adjusts the photogeneration current of lower bandgap sub-cells based to the operating point of the high bandgap cell above them. The IV of each sub-cell is then combined into a tandem IV based on the given tandem architecture according to a simple circuit model.

B. Energy yield calculation

Our global energy yield calculation routine is adopted and modified from the method developed by Peters et al [16]. Daily average values of operating environment parameters, including solar irradiance, ambient temperature, humidity, ground reflectance, and aerosol are taken from NASA's various satellite instruments in the Earth Observing System [17–19]. The solar spectrum is calculated with Simple Model of the Atmospheric Radiative Transfer of Sunshine (SMARTS) [20]. We describe the worldwide outdoor field performance by both energy yield and implied PR [21], i.e. the ratio of harvesting efficiency and STC efficiency.

III. Results and Discussions

A. Global outdoor field performance

In Figure 2, we show the predicted worldwide PR and energy yield for tandem modules with perovskite and GaAs top cells and a silicon bottom cell in the 3T architecture. In general, the highest PR is achieved in cold regions close to the poles or in high altitude. The perovskite on silicon tandem shows an overall larger variation across the globe than GaAs, which can be explained by the lower global PR variation of GaAs [22]. PR suffers in most parts of the tropics, largely due to significantly more blue-rich spectra resulting from low air mass and high water content [23, 24]. In these regions, customization of design may be needed. Energy yield variations follow PR variations with the additional influence of the different solar cell efficiencies.

B. Performance in different climate zones

Figure 3 shows the area-weighted distribution of PRs of GaAs and perovskite on silicon PV modules for three different climate zones. Comparing across tandem architectures, a few observations can be made. In general, 4T tandems have the highest PR, as expected. Remarkably, the PR of VM tandems is quite close to that of 4T in all climate zones, with an absolute difference of only 0.015 or less on average for perovskite-Si, and even a slight gain for GaAs-Si. This is possible because the voltage is not exactly matched at the maximum power point under STC. Therefore, when conditions change, the matching may improve over STC. Overall, it turns out that the voltage mismatch loss created by elevated temperatures is not significant for the investigated material systems. Therefore, with the same installed capacity, VM tandem module can deliver energy yield over 98% of what is achievable by 4T. This may be further improved by module level power electronics [4].

2T and AM tandems are of a similar type, in the sense that they are both current matched. Not surprisingly, they have similar PRs, and as a group, their PR is noticeably lower than that of the 4T or VM tandems, due to the sensitivity to spectral variations. Their PR is generally lower than 4T by 0.02 to 0.05. Nonetheless, in temperate and arid climates, all double-junction tandems can reach similar (>97%) performance ratio levels as SJ Si, agreeing with literature findings for specific locations [25, 26].

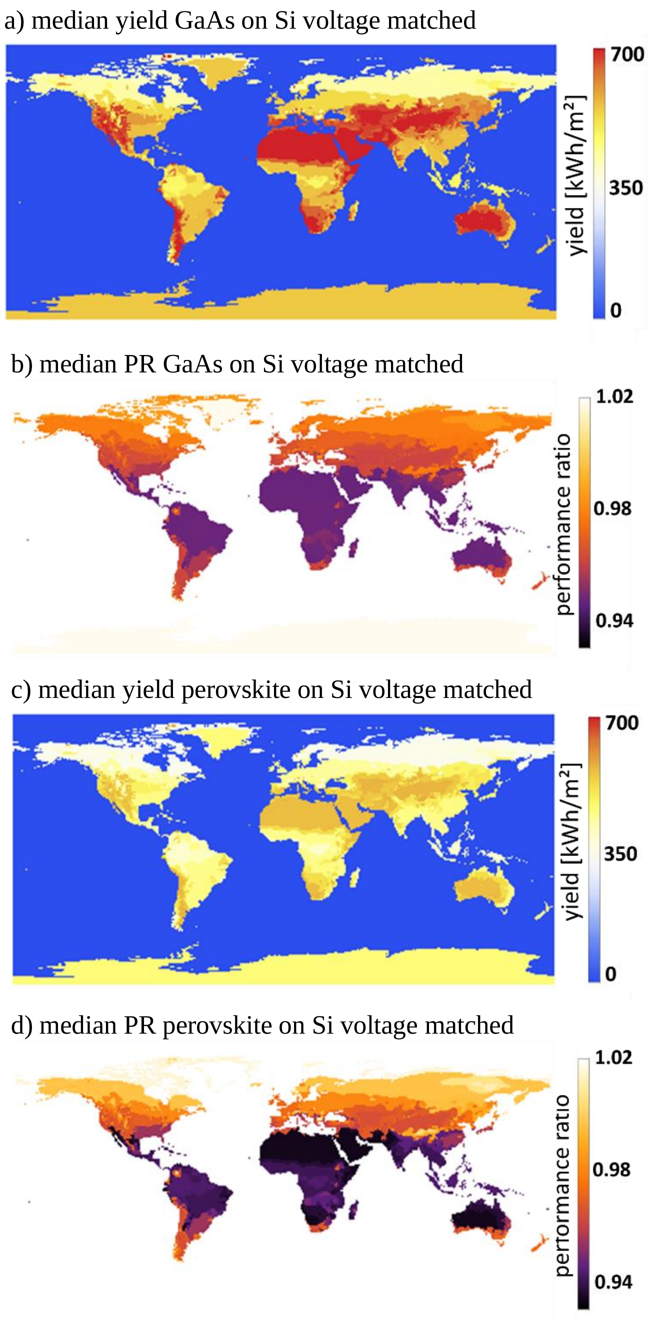

Figure 2. Energy yield (a,c) and PR (b,d) for GaAs on silicon and perovskite on Si tandem PV modules worldwide, both in the 3T/VM configuration.

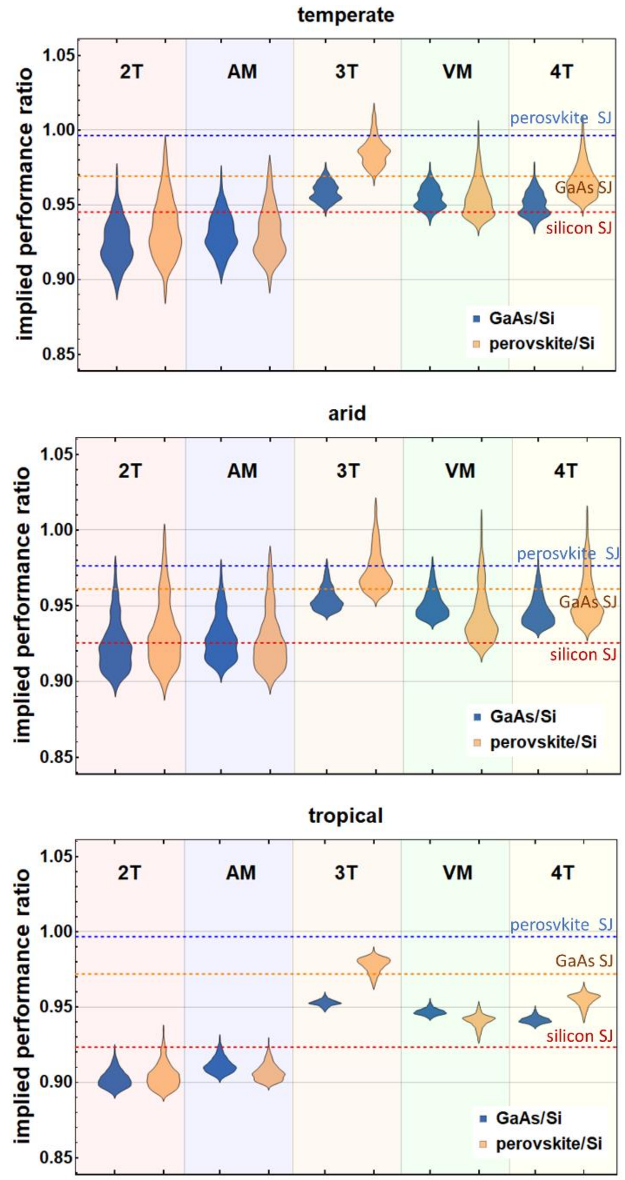

Figure 2. Distribution of calculated PRs for two tandem technologies: GaAs on silicon and perovskite on silicon for each tandem architecture and in three climate zones, termperate, arid and tropical.

C. Cost considerations

Figure 4 shows the calculated worldwide cost premium of a 34.2% efficient 4T GaAs-Si tandem PV module. In this exercise, we take into consideration the final yield, the module fabrication costs, and various other cost factors taken from the residential PV scenario [27].

In most areas, all tandems allow doubling the current level of Si module fabrication cost (100% cost premium). For 4T and 3T/VM, tripling of manufacturing cost is allowed in most places. Most promising regions for tandems include Australia, the Southern US, and the Middle East. Canada, Japan, New Zealand, and western half of Europe also allow high cost premium due to high installation and maintenance costs. This indicates that there is some room for tandems to compete with SJ Si in high-value residential markets, corroborating the conclusion from previous studies [28, 29].

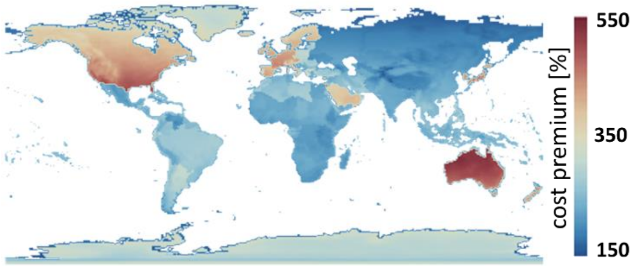

Figure 3. Calculated worldwide cost premium [13].

IV. Conclusions

In this work, we investigated the worldwide outdoor performance potential of five tandem module architectures with a variety of material combinations, including GaAs on silicon and perovskite on silicon, and the implications on cost competitiveness. In most parts of the world, the high efficiency of tandems is proportionally translated into superior yield. Most notably, we observe that the choice of the best tandem architecture depends on the characteristic of the sub-cells and operating conditions: if a tandem module with other architectures could be made at the same STC efficiency as a 4T module (despite imperfect current or voltage matching), it is possible to outperform the 4T module in the field. In general, our calculation indicates the voltage matching architectures (3T and mechanically voltage-matched tandem) to be promising candidates for achieving superior outdoor performance if they can indeed achieve good STC efficiency. With the same installed capacity, 3T and voltage-matched tandem modules deliver nearly equal (>98%), or even more than the power that is achievable by 4T tandems, which is commonly regarded as the ideal tandem in terms of yield. In addition, we investigate the boundary conditions for tandem modules to be economically successful. It is found that even for the same module configuration, its economic competitiveness differs significantly in different climates and geolocations. Tandem technology is potentially promising for future residential applications, and may even become viable for large scale installations, especially in high-value markets from arid climates.

Acknowledgment

This work was supported by the Solar Energy Research Institute of Singapore (SERIS) and the Singapore-MIT Alliance for Research and Technology (SMART). SERIS is supported by the National University of Singapore (NUS) and Singapore's National Research Foundation (NRF) through the Singapore Economic Development Board (EDB). We would also like to acknowledge NASA as the source of satellite data. This work was supported by the Bavarian State Government (project ''PV-Tera—Reliable and cost-efficient photovoltaic power generation on the Terawatt scale,'' no. 44- 6521a/20/5).

References

[1] S. Essig et al., "Raising the one-sun conversion efficiency of III–V/Si solar cells to 32.8% for two junctions and 35.9% for three junctions", *Nature Energy* 2 (2017), 17144.

[2] A. Al-Ashouri et al., "Monolithic perovskite/silicon tandem solar cell with >29% efficiency by enhanced hole extraction", *Science* 370 (2020), 1300-1309."

[3] J. Yang, Z. Peng, D. Cheong, and R. N. Kleiman, "III-V on Silicon Multi-Junction Solar Cell with 25% 1-Sun Efficiency via Direct Metal Interconnect and Areal Current Matching," in *27th European Photovoltaic Solar Energy Conference and Exhibition*, 2012, pp. 160–163, doi: 10.4229/27thEUPVSEC2012-1BO.12.6.

[4] S. MacAlpine *et al.*, "Simulated potential for enhanced performance of mechanically stacked hybrid III–V/Si tandem photovoltaic modules using DC–DC converters," *Journal of Photonics for Energy*, vol. 7, no. 4, pp. 1-11,11, 2017, [Online]. Available: https://doi.org/10.1117/1.JPE.7.042501.

[5] M. H. Futscher and B. Ehrler, "Efficiency Limit of Perovskite/Si Tandem Solar Cells," *ACS Energy Letters*, vol. 1, no. 4, pp. 863–868, 2016, doi: 10.1021/acsenergylett.6b00405.

[6] J. M. Gee, "A comparison of different module configurations for multi-band-gap solar cells," *Solar Cells*, vol. 24, no. 1–2, pp. 147–155, 1988, doi: 10.1016/0379-6787(88)90044-0.

[7] J. M. Gee, "A comparison of different module configurations for multi-band-gap solar cells," *Solar Cells*, vol. 24, no. 1–2, pp. 147–155, 1988, doi: http://dx.doi.org/10.1016/0379-6787(88)90044-0.

[8] E. L. Warren, M. G. Deceglie, M. Rienacker, R. Peibst, A. C. Tamboli, and P. Stradins, "Maximizing tandem solar cell power extraction using a three-terminal design," *Sustainable Energy & Fuels*, vol. 2, no. 6, pp. 1141–1147, 2018, doi: 10.1039/C8SE00133B.

[9] M. Rienäcker *et al.*, "Back-contacted bottom cells with three terminals: Maximizing power extraction from current-mismatched tandem cells," *Progress in Photovoltaics: Research and Applications*, vol. 27, no. 5, pp. 410–423, May 2019, doi: 10.1002/pip.3107.

[10] H. Schulte-Huxel, D. J. Friedman, and A. C. Tamboli, "String-Level Modeling of Two, Three, and Four Terminal Si-Based Tandem Modules," *IEEE Journal of Photovoltaics*, vol. 8, no. 5, pp. 1370–1375, Sep. 2018, doi: 10.1109/JPHOTOV.2018.2855104.

[11] M. A. Steiner *et al.*, "A monolithic three-terminal GaInAsP/GaInAs tandem solar cell," *Progress in Photovoltaics: Research and Applications*, vol. 17, no. 8, pp. 587–593, Dec. 2009, doi: 10.1002/pip.913.

[12] M. Emziane and R. J. Nicholas, "Double-junction three-terminal photovoltaic devices: A modeling approach," *Journal of Applied Physics*, vol. 102, no. 7, 2007, doi: 10.1063/1.2786614.

[13] H. Liu, C. D. Rodríguez-Gallegos, Z. Liu, T. Buonassisi, T. Reindl, I. M. Peters, "A worldwide theoretical comparison of outdoor potential for various silicon-based tandem module architecture" *Cell Reports Physical Science* 1 (2020), 100037.

[14] J. F. Geisz *et al.*, “Generalized Optoelectronic Model of Series-Connected Multijunction Solar Cells,” *IEEE Journal of Photovoltaics*, vol. 5, no. 6, pp. 1827–1839, 2015, doi: 10.1109/JPHOTOV.2015.2478072.

[15] Z. Liu *et al.*, “A modeling framework for optimizing current density in four-terminal tandem solar cells: A case study on GaAs/Si tandem,” *Solar Energy Materials and Solar Cells*, vol. 170, pp. 167–177, Oct. 2017, doi: 10.1016/j.solmat.2017.05.048.

[16] I. M. Peters, H. Liu, T. Reindl, and T. Buonassisi, “Global Prediction of Photovoltaic Field Performance Differences Using Open-Source Satellite Data,” *Joule*, vol. 2, no. 2, pp. 307–322, Feb. 2018, doi: 10.1016/j.joule.2017.11.012.

[17] NASA, “Clouds and Earth’s Radiant Energy System (CERES),” 2018. https://ceres.larc.nasa.gov/.

[18] NASA, “Atmospheric Infrared Sounder (AIRS),” 2018. https://airs.jpl.nasa.gov/.

[19] NASA, “Moderate Resolution Imaging Spectroradiometer (MODIS),” 2018. https://modis.gsfc.nasa.gov/.

[20] C. Gueymard and F. S. E. Center, “SMARTS2: a simple model of the atmospheric radiative transfer of sunshine: algorithms and performance assessment,” 1995. [Online]. Available: http://www.fsec.ucf.edu/en/publications/pdf/FSEC-PF-270-95.pdf.

[21] H. Liu, Z. Ren, Z. Liu, A. G. Aberle, T. Buonassisi, and I. M. Peters, “Predicting the outdoor performance of flat-plate III–V/Si tandem solar cells,” *Solar Energy*, vol. 149, pp. 77–84, 2017, doi: 10.1016/j.solener.2017.04.003.

[22] I. M. Peters, and T. Buonassisi, “Energy yield limits for single-junction solar cells,” *Joule* 2 (2018), 1160-1170.

[23] H. Liu, Z. Ren, Z. Liu, A. G. Aberle, T. Buonassisi, and I. M. Peters, “The realistic energy yield potential of GaAs-on-Si tandem solar cells: a theoretical case study,” *Optics Express*, vol. 23, no. 7, p. A382, Apr. 2015, doi: 10.1364/oe.23.00a382.

[24] H. Liu, A. G. Aberle, T. Buonassisi, and I. M. Peters, “On the methodology of energy yield assessment for one-Sun tandem solar cells,” *Solar Energy*, vol. 135, pp. 598–604, Oct. 2016, doi: 10.1016/j.solener.2016.06.028.

[25] M. H. Futscher and B. Ehrler, “Modeling the Performance Limitations and Prospects of Perovskite/Si Tandem Solar Cells under Realistic Operating Conditions,” *ACS Energy Letters*, vol. 2, no. 9, pp. 2089–2095, Sep. 2017, doi: 10.1021/acsenergylett.7b00596.

[26] B. C. Duck *et al.*, “Energy yield potential of perovskite-silicon tandem devices,” in *43rd IEEE Photovoltaic Specialists Conference (PVSC)*, 2016, pp. 1624–1629, doi: 10.1109/PVSC.2016.7749896.

[27] F. Fu, D. Feldman, and R. Margolis, “U.S. Solar Photovoltaic System Cost Benchmark: Q1 2018,” National Renewable Energy Laboratory, 2018.

[28] Z. J. Yu, J. v. Carpenter, and Z. C. Holman, “Techno-economic viability of silicon-based tandem photovoltaic modules in the United States,” *Nature Energy*, vol. 3, no. 9, pp. 747–753, Sep. 2018, doi: 10.1038/s41560-018-0201-5.

[29] S. E. Sofia, J. P. Mailoa, D. N. Weiss, B. J. Stanbery, T. Buonassisi, and I. M. Peters, “Economic viability of thin-film tandem solar modules in the United States,” *Nature Energy*, vol. 3, no. 5, pp. 387–394, 2018, doi: 10.1038/s41560-018-0126-z.